

# Fe<sub>3</sub>O<sub>4</sub>@chitosan nanoparticles: a valuable heterogeneous nanocatalyst for the synthesis of 2,4,5-trisubstituted imidazoles

Cite this: *RSC Adv.*, 2014, 4, 20932

Zohre Zarnegar and Javad Safari\*

Chitosan-coated Fe<sub>3</sub>O<sub>4</sub> nanoparticles (Fe<sub>3</sub>O<sub>4</sub>@CS) were prepared simply through *in situ* co-precipitation of Fe<sup>2+</sup> and Fe<sup>3+</sup> ions *via* NH<sub>4</sub>OH in an aqueous solution of chitosan and their catalytic activity was investigated in the synthesis of 2,4,5-trisubstituted imidazoles by a one-pot condensation of benzil derivatives, aryl aldehydes and ammonium acetate in EtOH. This novel method offers several advantages compared to those reported in the previous literature, including avoiding the use of harmful catalysts, easy and quick isolation of the products, excellent yields, mild and clean conditions, and simplicity of the methodology. High catalytic activity and ease of recovery using an external magnetic field are additional eco-friendly attributes of this catalytic system.

Received 8th April 2014  
Accepted 25th April 2014

DOI: 10.1039/c4ra03176h

[www.rsc.org/advances](http://www.rsc.org/advances)

## 1. Introduction

Imidazole derivatives are a class of heterocyclic compounds that contain nitrogen and are currently under intensive focus due to their wide range of applications, because they have many pharmacological properties and play important roles in biochemical processes.<sup>1,2</sup> The imidazole compounds are known to possess NO synthase inhibition and antifungal, antibiotic, antimycotic, antiulcerative, antitumor, antibacterial, and CB1 receptor antagonistic activities.<sup>3,4</sup> Various substituted imidazoles act as inhibitors of p38 MAP kinase<sup>5</sup> and B-Raf kinase,<sup>6</sup> plant growth regulators,<sup>7</sup> glucagon receptors,<sup>8</sup> pesticides,<sup>9</sup> and therapeutic agents.<sup>10</sup> Thus, synthesis of these important heterocyclic nucleus have rekindled our interest in obtaining trisubstituted imidazole. Accordingly, a number of synthetic methods have been reported for the synthesis of 2,4,5-trisubstituted imidazoles. These methods involve condensation of aldehyde, benzil and ammonium acetate by using various catalytic systems.<sup>11–18</sup> Owing to the wide range of pharmacological and biological activities, the development of economical, effective, clean, high-yielding and mild environmental benign protocols is still desirable and is in demand. Moreover, the design of efficient, valuable, and recoverable catalysts is important for both economical and environmental points of view.

In recent decade, magnetic nanoparticles (MNPs) have appeared as an excellent type of catalyst support because of their good stability, easy synthesis and functionalization, high surface area and facile separation by magnetic forces, as well as

low toxicity and price.<sup>19</sup> Other important features of these magnetic catalysts are high catalytic activity, simple magnetic separation of them using an external magnet, high degree of chemical stability in various organic and inorganic solvents, reusability and benign character in the context of green chemistry. As a result, magnetically recyclable nanocatalyst systems have enabled researchers to apply nanocatalysts as greener and sustainable options for organic transformations.<sup>20</sup>

On the other hand, recently biopolymers such as cellulose,<sup>21</sup> starch,<sup>22</sup> chitosan (CS)<sup>20,23</sup> or wool<sup>24</sup> have been used as heterogeneous catalytic systems. In this context, chitosan can play a major role as a natural, biocompatible, and biodegradable polymer. Literature survey shows that a wide range of applications have been reported for chitosan in different fields such as drug delivery, cosmetics, water treatment, food packaging, fuel cells, membranes, hydrogels, surface conditioners, and catalyst.<sup>25</sup> Chitosan as a polyaminosaccharide, can be explored as a mild bifunctional heterogeneous catalyst in organic reactions. In this regard, chitosan contains both amino groups and primary and secondary hydroxyl groups in higher concentrations. Therefore, chitosan can activate the electrophilic and nucleophilic components of the reactions by hydrogen bonding and lone pairs, respectively.<sup>23a</sup>

Herein we wish to report a new efficient and practical route for the one-pot three-component synthesis of trisubstituted imidazoles by the condensation of benzil derivatives, aryl aldehydes and ammonium acetate catalyzed by Fe<sub>3</sub>O<sub>4</sub>@CS nanoparticles. This new approach has several superiorities *versus* previous reports for the synthesis of highly substituted imidazole derivatives and opens an important field to the use of magnetically recoverable and environmentally benign heterogeneous nanocatalyst in the synthesis of pharmaceutically important heterocyclic compounds (Scheme 1).

Laboratory of Organic Compound Research, Department of Organic Chemistry, College of Chemistry, University of Kashan, P.O. Box: 87317-51167, Kashan, I.R. Iran. E-mail: Safari@kashanu.ac.ir; safari\_jav@yahoo.com; Fax: +98 361 5912397; Tel: +98 361 591 2320



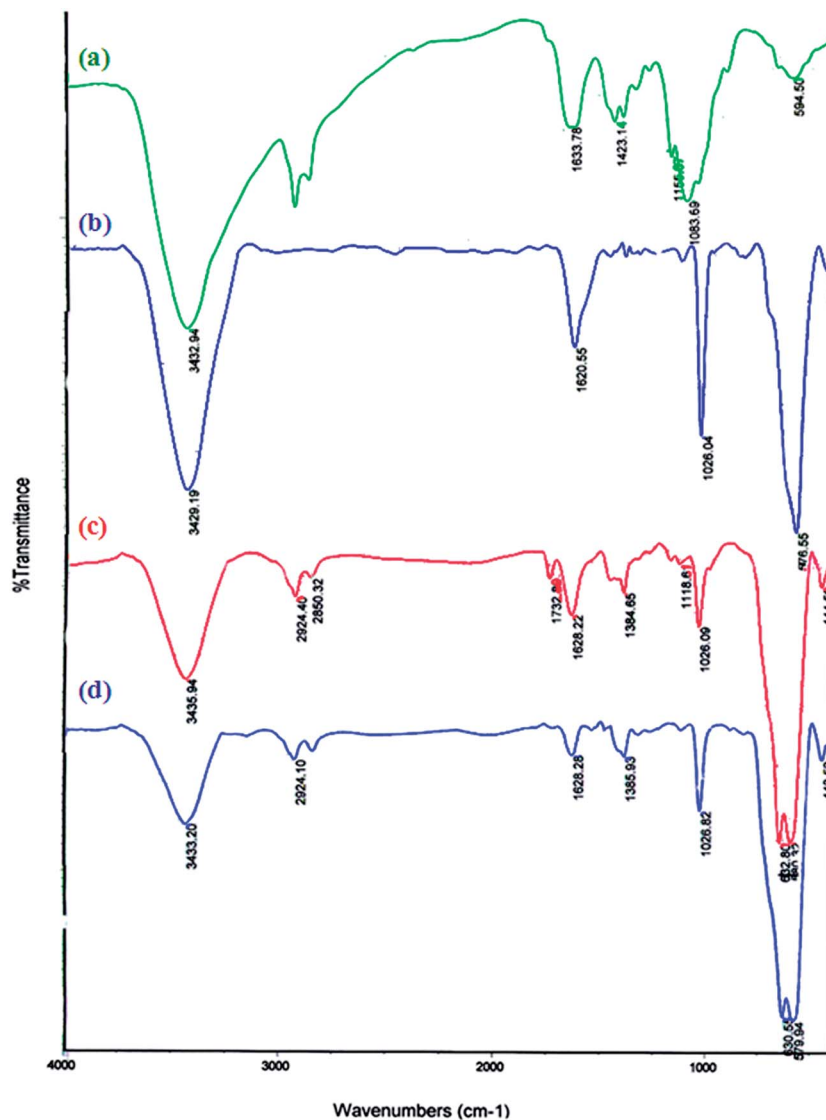


Fig. 1 IR spectra of (a) chitosan, (b) Fe<sub>3</sub>O<sub>4</sub>, (c) Fe<sub>3</sub>O<sub>4</sub>@CS and (d) recovered Fe<sub>3</sub>O<sub>4</sub>@chitosan.

As illustrated in Fig. 4, the particle size was studied by scanning electron microscopy (SEM) and the identification of Fe<sub>3</sub>O<sub>4</sub>@chitosan was based on the analysis of SEM images. The obtained SEM images of nanoparticles clearly showed that Fe<sub>3</sub>O<sub>4</sub> nanoparticles were properly supported on chitosan.

Magnetic measurements of Fe<sub>3</sub>O<sub>4</sub> and Fe<sub>3</sub>O<sub>4</sub>@chitosan nanoparticles were investigated with VSM. The hysteresis loops of Fe<sub>3</sub>O<sub>4</sub> and Fe<sub>3</sub>O<sub>4</sub>@chitosan nanoparticles are shown in Fig. 5. It can be seen that both materials show ferromagnetic behavior. The magnetic saturation values of Fe<sub>3</sub>O<sub>4</sub> MNPs and Fe<sub>3</sub>O<sub>4</sub>@chitosan nanoparticles are 66.58 and 20.17 emu g<sup>-1</sup>, respectively. The decrease in magnetic saturation for Fe<sub>3</sub>O<sub>4</sub>@chitosan is attributed to the cover of chitosan polymeric matrix on the surface of magnetic Fe<sub>3</sub>O<sub>4</sub> MNPs.<sup>28</sup> However, such a magnetic property is strong enough for the as-prepared Fe<sub>3</sub>O<sub>4</sub>@chitosan to be easily separated from EtOH under a magnetic field. The magnetic effect of Fe<sub>3</sub>O<sub>4</sub>@chitosan under an external magnetic field is shown in Fig. 6. Clearly, the Fe<sub>3</sub>O<sub>4</sub>@chitosan can be

easily and quickly separated from the reaction mixture with the help of an external magnet, which proves that magnetic property of the Fe<sub>3</sub>O<sub>4</sub>@chitosan as nanocatalyst is strong enough for easy recovery and reuse from the reaction mixture.

To show the efficiency of the Fe<sub>3</sub>O<sub>4</sub>@chitosan as magnetic catalyst, initially, we sought a mild and convenient method for the synthesis of 2,4,5-trisubstituted imidazole derivatives at heating condition. Our investigation began with the evaluation of Fe<sub>3</sub>O<sub>4</sub>@chitosan as heterogeneous catalyst in the reaction of benzaldehyde (1 mmol), benzil (1 mmol) and ammonium acetate (5 mmol) as model reaction. The use of 0.05 g of Fe<sub>3</sub>O<sub>4</sub>@chitosan as nanocatalyst in EtOH afforded a 95% yield (Table 1, entry 4) of the desired product **4a**. Among the tested solvents such as chloroform, dichloromethane, methanol, ethanol, and acetonitrile, the formation of product **4a** was more facile and proceeded to give highest yield, in EtOH as solvent. The results indicated that the yield gradually decreased as we moved from highly polar to less polar solvents. To evaluate and

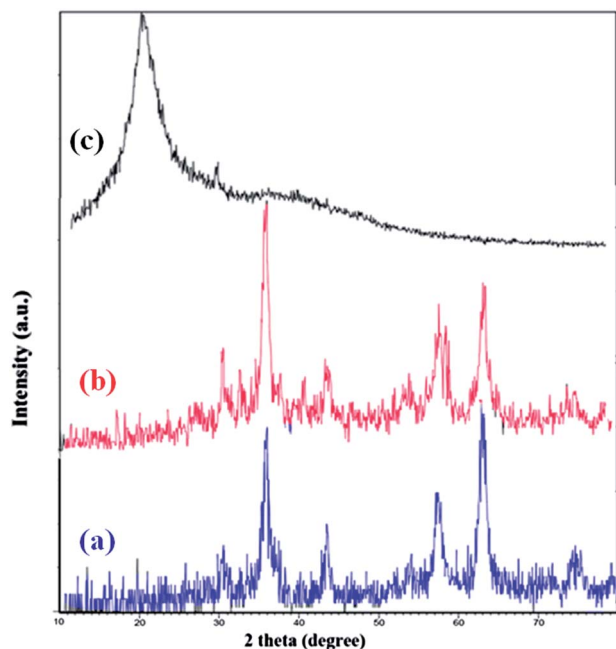


Fig. 2 XRD patterns of the (a)  $\text{Fe}_3\text{O}_4$  MNPs, (b)  $\text{Fe}_3\text{O}_4$ @CS nanocomposite and (c) chitosan.

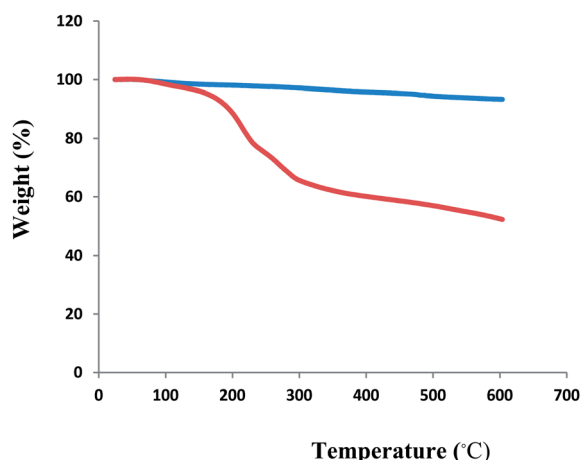


Fig. 3 TGA curves for (a) uncoated MNPs and (b)  $\text{Fe}_3\text{O}_4$ @chitosan nanocomposite.

optimize the catalytic system, one-pot condensation to give **4a** was examined with  $\text{Fe}_3\text{O}_4$ , chitosan  $\text{Fe}_3\text{O}_4$ @chitosan as catalyst (Table 1). Interestingly, it was found that  $\text{Fe}_3\text{O}_4$ @chitosan was proved to be an efficient catalyst and gave exclusively 1-(phenyl)-2,4,5-triphenylimidazole **4a** in 95% yield in 2 h under reflux conditions (Table 1). As Table 1 shows, initial screening studies identified that all the above-mentioned catalysts shows a good catalytic activity for the model reaction but  $\text{Fe}_3\text{O}_4$ @chitosan exhibited highest catalytic activity as compared with  $\text{Fe}_3\text{O}_4$  and chitosan. We believe that this composite has two active components for catalytic activity containing chitosan and magnetite. With notice to these results,  $\text{Fe}_3\text{O}_4$ @chitosan were chosen as the best catalyst for further work.

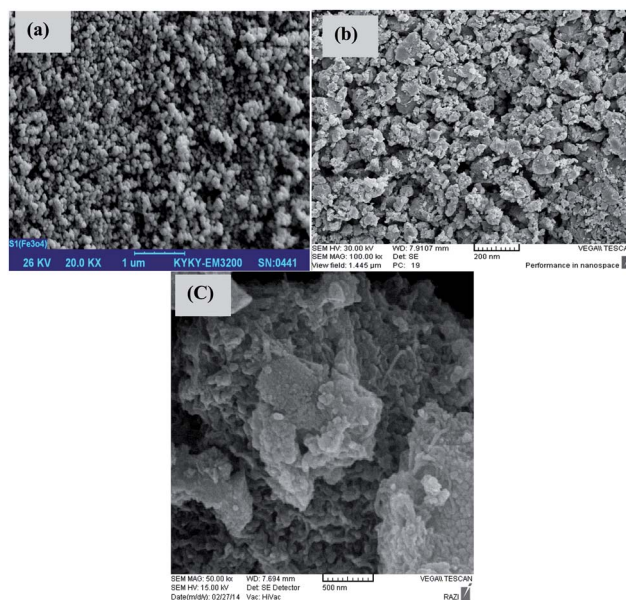


Fig. 4 SEM morphology of (a) unmodified  $\text{Fe}_3\text{O}_4$  magnetic nanoparticles, (b)  $\text{Fe}_3\text{O}_4$ @chitosan nanocomposite and (c)  $\text{Fe}_3\text{O}_4$ @chitosan after being used 6 times.

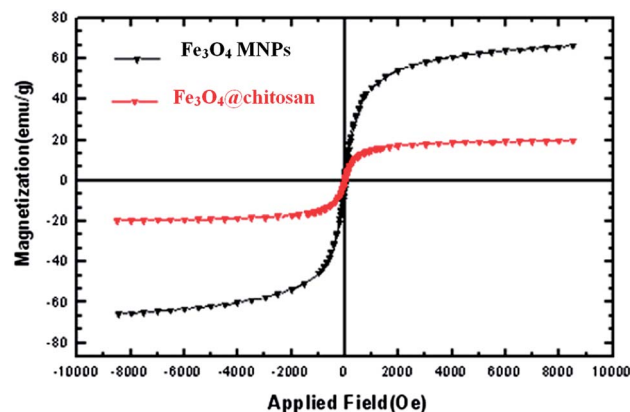


Fig. 5 Magnetization curves for the  $\text{Fe}_3\text{O}_4$  MNPs and  $\text{Fe}_3\text{O}_4$ @chitosan nanocomposite at room temperature.

We next examined a wide variety of aldehydes and 1,2-diketones to establish the scope of this catalytic transformation (Table 2). Various aromatic aldehydes bearing electron donating and electron withdrawing substituents underwent this cyclocondensation to furnish trisubstituted imidazoles in high yields. Also, benzil derivatives afforded the corresponding imidazoles in high yields. In general, this synthetic protocol was clean and no side products were detected. In all cases, the reactions proceeded efficiently under mild conditions. The results reveal that the unique heterogeneous  $\text{Fe}_3\text{O}_4$ @chitosan nanoparticles appears as an effective catalyst which produces high yields through a simple procedure.

The structure of trisubstituted imidazoles **4a-I** was deduced from their high-field  $^1\text{H}$  NMR, IR, Rf, and UV spectral data. Also,

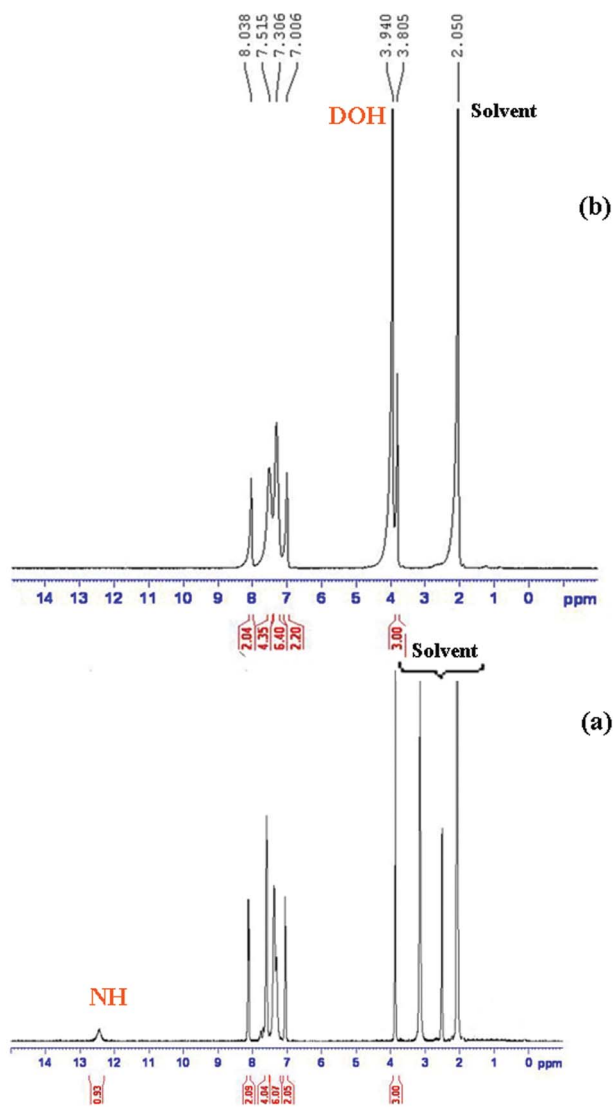


Fig. 6  $^1\text{H}$  NMR spectra of 2-(4-methoxyphenyl)-4,5-diphenyl-1*H*-imidazole (**4b**) in (a) acetone +  $\text{DMSO}-d_6$  and (b) acetone +  $\text{D}_2\text{O}$ .

Table 1 Effect of the amount of  $\text{Fe}_3\text{O}_4$ @chitosan nanoparticles and solvents on the synthesis of compound **4a** under reflux condition

Entry	Catalyst (g)	Solvent	Time (h)	Yield (%)
1	—	EtOH	5	15
2	$\text{Fe}_3\text{O}_4$ @chitosan (0.03)	EtOH	3	60
3	$\text{Fe}_3\text{O}_4$ @chitosan (0.04)	EtOH	2	72
4	$\text{Fe}_3\text{O}_4$ @chitosan (0.05)	EtOH	2	95
5	$\text{Fe}_3\text{O}_4$ @chitosan (0.06)	EtOH	2	94
6	$\text{Fe}_3\text{O}_4$ (0.05)	EtOH	2	70
7	Chitosan (0.05)	EtOH	2	80
8	$\text{Fe}_3\text{O}_4$ @chitosan (0.05)	MeOH	3	90
9	$\text{Fe}_3\text{O}_4$ @chitosan (0.05)	Acetonitrile	3	70
10	$\text{Fe}_3\text{O}_4$ @chitosan (0.05)	Chloroform	5	55
11	$\text{Fe}_3\text{O}_4$ @chitosan (0.05)	Dichloromethane	5	40

their melting points were compared with literature reports.  $^1\text{H}$  NMR spectra for compound **4b** is given in Fig. 6. In the  $^1\text{H}$  NMR spectra Fig. 6(a), the signal around  $\delta = 3.85$  ppm corresponding

to methoxy group. In this figure, the signals of aromatic protons can be seen at  $\delta = 7.4$ – $8.1$  ppm. The signal around  $\delta = 12.5$  ppm is related to the NH proton. Presence of this signal confirmed the formation of desired products in this reaction. To prove NH group, we have investigated hydrogen–deuterium exchange protocol for compound **4b** (Fig. 6(b)). In this method, a drop of  $\text{D}_2\text{O}$  is placed in the NMR tube containing the acetone solution of the compound **4b**. After shaking a sample and sitting for a few minutes, the NH hydrogen is replaced deuterium, causing it to disappear from the spectrum at  $\delta = 12.5$  ppm.

A plausible mechanism for this reaction catalyzed by  $\text{Fe}_3\text{O}_4$ @chitosan is shown in Scheme 3. In the case of trisubstituted imidazole the reaction proceeds through diamine intermediate A. The aldehydic carbonyl oxygen are activated by  $\text{Fe}_3\text{O}_4$  ( $\text{Fe}^{+3}$  and  $\text{Fe}^{+2}$ ) and chitosan supported magnetic nanoparticles and subsequent condensation with two molecules of ammonia to form diamine intermediate A. The free hydroxyl and amino groups distributed on the surface of chitosan supported  $\text{Fe}_3\text{O}_4$  in high concentrations activate the carbonyl group of the aldehyde.<sup>23a</sup> Condenses with the carbonyl carbons of the 1,2-diketone followed by dehydration to afford the imino intermediate B, which rearranges to the required trisubstituted imidazoles.<sup>1</sup>

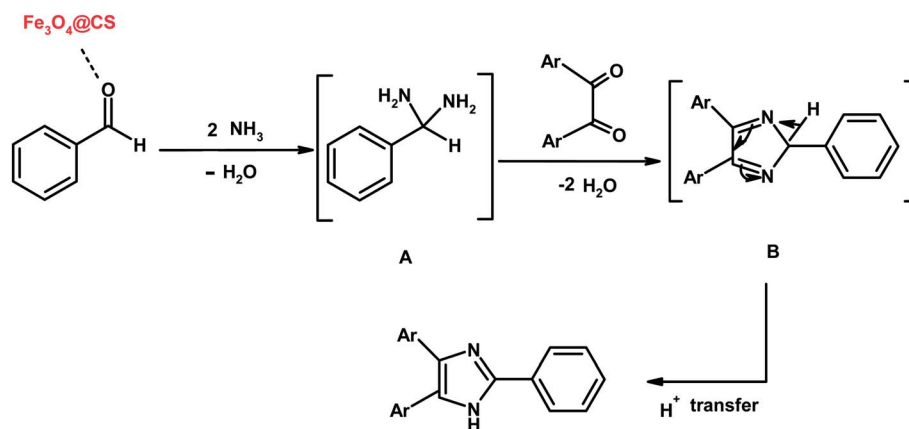
One of the advantages of this active, non-toxic, and environmentally benign heterogeneous bio-polymer catalyst is its ability to perform as a recyclable reaction medium. In a typical procedure, after completion of the reaction, the magnetic nanocatalyst is easily and efficiently separated from the product by attaching an external magnet to the reaction vessel, followed by simple decantation of the reaction solution (Fig. 7). The recycled catalyst could be reused six times without great loss of catalytic activity (Fig. 8). The recovered nanocatalyst was characterized with FT-IR spectroscopy (Fig. 1(d)). In IR spectrum, the band from  $580\text{ cm}^{-1}$  is assigned to the stretching vibrations of (Fe–O) bond in  $\text{Fe}_3\text{O}_4$ , and the band at about  $1027\text{ cm}^{-1}$  is belong to the stretching of the (C–O) bond. The coated cross-linked chitosan ensured the stability of the  $\text{Fe}_3\text{O}_4$  core during the catalytic process, so as to obtain a high recyclability. After 6 times of reuse, chitosan may be destroyed and  $\text{Fe}_3\text{O}_4$  having lost the protection of chitosan was easy to aggregate (as shown in SEM image Fig. 4(c)) or oxidize. There for, the catalyst would be lost in the solution and recovery efficiency decreased gradually.<sup>23b</sup>

### 3. Conclusions

In summary, a new, simple, efficient and environmentally benign method for the synthesis of 2,4,5-trisubstituted imidazoles by the use of renewable and heterogeneous  $\text{Fe}_3\text{O}_4$ @chitosan as magnetic biocatalyst has been described. Clean reaction profiles, excellent yields, the use of a one-pot and multicomponent procedure for the synthesis of imidazoles, reusability of the catalyst, practicability, and operational simplicity are the important features of this methodology.

Table 2 One-pot synthesis of 2,4,5-trisubstituted imidazoles catalyzed by  $\text{Fe}_3\text{O}_4@\text{chitosan}$  under reflux condition

Entry	$R_1, R_2$	$R_3$	Product	Time (h)	Yield (%)	$\text{mp}_{\text{rep.}}/\text{mp}_{\text{lit.}}$ ( $^{\circ}\text{C}$ )
1	H	H	4a	2	95	(271–273)/(270–272) [ref. 29]
2	H	<i>p</i> -OMe	4b	3	90	(230–231)/(228–231) [ref. 29]
3	H	<i>m</i> -OMe, <i>p</i> -OMe	4c	2	92	(214–216)/213–216 [ref. 30]
4	H	<i>p</i> -Cl	4d	2.5	96	(260–262)/(260–261) [ref. 30]
5	H	<i>m</i> -OMe	4e	2.5	98	(258–260)/(259–262) [ref. 29]
6	H	2-Naphthyl	4f	2.5	98	(274–275)/(273–276) [ref. 30]
7	H	<i>m</i> -OMe, <i>m</i> -OMe	4g	3.5	98	(255–257)/(254–256) [ref. 30]
8	OMe	H	4h	3	95	(202–204)/(201–203) [ref. 29]
9	OMe	<i>p</i> -OMe	4i	3.5	90	(184–186)/(183–185) [ref. 29]
10	OMe	2-Naphthyl	4j	3	95	(228–230)/(228–230) [ref. 31]
11	F	<i>m</i> -OMe, <i>p</i> -OMe	4k	1	98	(206–208)/(207–208) [ref. 30]
12	F	2-Naphthyl	4l	1	98	(273–275)/(273–275) [ref. 31]



Scheme 3 Plausible mechanism of the reaction.



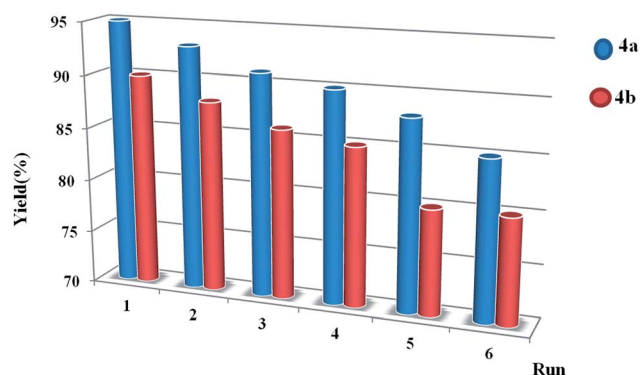
Fig. 7 Separation of the nanocatalyst from the reaction mixture by an external magnet.

## 4. Experimental

### 4.1. Chemicals and apparatus

All reagents were purchased from Merck and Aldrich and used without further purification. Melting points were determined in open capillaries using an Electrothermal Mk3 apparatus and are uncorrected.  $^1\text{H}$  NMR and  $^{13}\text{C}$  NMR spectra were recorded

with a Bruker DRX-400 spectrometer at 400 and 100 MHz respectively. NMR spectra were obtained in  $\text{DMSO-}d_6$  and acetone solutions and are reported as parts per million (ppm) downfield from tetramethylsilane as internal standard. Fourier transform infrared spectroscopy (FT-IR) spectra were obtained with potassium bromide pellets in the range  $400\text{--}4000\text{ cm}^{-1}$  with a Perkin-Elmer 550 spectrometer. The UV-vis measurements were obtained with a GBC cintra 6 UV-vis spectrophotometer. Nanostructures were characterized using a Holland

Fig. 8 Reusability of  $\text{Fe}_3\text{O}_4@\text{chitosan}$  for the synthesis of 4a and 4b.

Philips Xpert X-ray powder diffraction (XRD) diffractometer (CuK $\alpha$ , radiation,  $\lambda = 0.154056$  nm), at a scanning speed of  $2^\circ \text{ min}^{-1}$  from  $10^\circ$  to  $100^\circ$  ( $2\theta$ ). Scanning electron microscope (SEM) was performed on a FEI Quanta 200 SEM operated at a 20 kV accelerating voltage. The samples for SEM were prepared by spreading a small drop containing nanoparticles onto a silicon wafer and being dried almost completely in air at room temperature for 2 h, and then were transferred onto SEM conductive tapes. The transferred sample was coated with a thin layer of gold before measurement. The magnetic properties were characterized by a vibrating sample magnetometer (VSM, Lakeshore7407) at room temperature.

## 4.2. Preparation of the Fe<sub>3</sub>O<sub>4</sub>@CS

Fe<sub>3</sub>O<sub>4</sub>@CS nanoparticles were prepared using chemical coprecipitation described in the literature.<sup>26</sup> In short, 1.5 g of chitosan (molecular weight: 100 000–300 000) is dissolved in 100 mL of 0.05 M acetic acid solution; to which FeCl<sub>2</sub>·4H<sub>2</sub>O (1.29 g, 0.0065 mol) and FeCl<sub>3</sub>·6H<sub>2</sub>O (3.51 g, 0.013 mol) are added. The resulting solution is mechanically stirred for 6 h at 80 °C under Ar atmosphere. Subsequently, 6 mL of 25% NH<sub>4</sub>OH is injected dropwise into the reaction mixture with constant stirring. After 30 min, the mixture is cooled to room temperature and chitosan coated over magnetic nanoparticles were separated by magnetic decantation and washed three times with distilled water, then ethanol, and finally dried under vacuum at room temperature (Scheme 3).

## 4.3. General procedure for the synthesis of 2,4,5-trisubstituted imidazoles

A mixture of benzil (1 mmol), aldehyde (1 mmol), ammonium acetate (0.4 g, 5 mmol) and Fe<sub>3</sub>O<sub>4</sub>@CS (0.05 g) in 10 mL ethanol was taken in a 50 mL flask and the reaction mixture was stirred under reflux condition for the stipulated period of time. The progress of the reaction was monitored by TLC. After the reaction was completed, the catalyst was separated by an external magnet. The reaction mixture was concentrated on a rotary evaporator under reduced pressure and the solid product obtained was washed with water and recrystallized from acetone–water 9 : 1 (v/v) to produce the desired 2,4,5-trisubstituted imidazoles.

## 4.4. Product characterization data of 2,4,5-trisubstituted imidazoles

**4.4.1. 2,4,5-Triphenyl-1H-imidazole (4a, C<sub>21</sub>H<sub>16</sub>N<sub>2</sub>).** White powder;  $R_f$  (in petroleum ether : ethylacetate; 7 : 3(v/v)): 0.74; UV (CHCl<sub>3</sub>)  $\lambda_{\text{max}}$ (nm): 334; IR (KBr)  $\bar{\nu}$  (cm<sup>-1</sup>): 3434 (N–H), 1597 (C=C), 1490 (C=N), <sup>1</sup>H NMR (acetone + DMSO-*d*<sub>6</sub>, 400 MHz)  $\delta$  (ppm): 12.9 (s, 1H, N–H), 8.63 (d, 2H, <sup>3</sup>*J* = 7.9 Hz, Ar–H), 8.08–7.14 (m, 4H, Ar–H), 7.92 (m, 4H, Ar–H), 7.83 (t, <sup>3</sup>*J* = 8 Hz, 2H, Ar–H), 7.73 (t, <sup>3</sup>*J* = 7 Hz, 2H, Ar–H), 7.67 (t, <sup>3</sup>*J* = 8 Hz, 1H, Ar–H).

**4.4.2. 2-(4-Methoxyphenyl)-4,5-diphenyl-1H-imidazole (4b, C<sub>22</sub>H<sub>18</sub>N<sub>2</sub>O).** White powder;  $R_f$  (in petroleum ether : ethylacetate; 7 : 3(v/v)): 0.64; UV (CHCl<sub>3</sub>)  $\lambda_{\text{max}}$ (nm): 338; IR (KBr)  $\bar{\nu}$  (cm<sup>-1</sup>): 3432 (N–H), 1611 (C=C), 1494 (C=N), 1250 (C–O); <sup>1</sup>H NMR (acetone + DMSO-*d*<sub>6</sub>, 400 MHz)  $\delta$  (ppm): 12.5 (s,

1H, N–H), 8.12 (d, 2H, <sup>3</sup>*J* = 8.8 Hz, Ar–H), 7.58–7.59 (m, 4H, Ar–H), 7.30–7.36 (m, 6H, Ar–H), 7.04 (d, 2H, <sup>3</sup>*J* = 8.4 Hz, Ar–H), 3.85 (s, 3H, OCH<sub>3</sub>).

**4.4.3. 2-(3,4-Dimethoxyphenyl)-4,5-diphenyl-1H-imidazole (4c, C<sub>23</sub>H<sub>20</sub>N<sub>2</sub>O<sub>2</sub>).** White powder;  $R_f$  (in petroleum ether : ethylacetate; 7 : 3(v/v)): 0.23; UV (CHCl<sub>3</sub>)  $\lambda_{\text{max}}$ (nm): 350; IR (KBr)  $\bar{\nu}$  (cm<sup>-1</sup>): 3430 (N–H), 1600 (C=C), 1500 (C=N), 1257 (C–O); <sup>1</sup>H NMR (CDCl<sub>3</sub>, 400 MHz)  $\delta$  (ppm): 9.8 (s, 1H, N–H), 8.53–8.58 (m, 3H, Ar–H), 7.27–7.33 (m, 9H, Ar–H), 6.90 (d, 1H, <sup>3</sup>*J* = 7.6 Hz, Ar–H), 3.92 (s, 3H, OCH<sub>3</sub>), 3.89 (s, 3H, OCH<sub>3</sub>).

**4.4.4. 2-(4-Chlorophenyl)-4,5-diphenyl-1H-imidazole (4d, C<sub>21</sub>H<sub>15</sub>N<sub>2</sub>Cl).** White powder;  $R_f$  (in petroleum ether : ethylacetate; 7 : 3(v/v)): 0.86; UV (CHCl<sub>3</sub>)  $\lambda_{\text{max}}$ (nm): 348; IR (KBr)  $\bar{\nu}$  (cm<sup>-1</sup>): 3433 (N–H), 1602 (C=C), 1485 (C=N), <sup>1</sup>H NMR (CDCl<sub>3</sub>, 400 MHz)  $\delta$  (ppm): 9.6 (s, 1H, N–H), 7.83–7.85 (d, 2H, <sup>3</sup>*J* = 8.4 Hz, Ar–H), 7.56 (m, 4H, Ar–H), 7.41–7.43 (d, 2H, <sup>3</sup>*J* = 8.4 Hz, Ar–H), 7.27–7.37 (m, 6H, Ar–H).

**4.4.5. 2-(3-Methoxyphenyl)-4,5-diphenyl-1H-imidazole (4e, C<sub>22</sub>H<sub>18</sub>N<sub>2</sub>O).** White powder;  $R_f$  (in petroleum ether : ethylacetate; 7 : 3(v/v)): 0.37; UV (CHCl<sub>3</sub>)  $\lambda_{\text{max}}$ (nm): 346; IR (KBr)  $\bar{\nu}$  (cm<sup>-1</sup>): 3435 (N–H), 1591 (C=C), 1482 (C=N), 1241 (C–O); <sup>1</sup>H NMR (CDCl<sub>3</sub>, 400 MHz)  $\delta$  (ppm): 9.5 (s, 1H, N–H), 7.54 (m, 1H, Ar–H), 7.43–7.27 (m, 1H, Ar–H), 6.95 (d, 1H, <sup>3</sup>*J* = 8 Hz, Ar–H), 3.89 (s, 3H, OCH<sub>3</sub>).

**4.4.6. 2-(2-Naphthyl)-4,5-diphenyl-1H-imidazole (4f, C<sub>28</sub>H<sub>18</sub>N<sub>2</sub>).** White powder;  $R_f$  (in petroleum ether : ethylacetate; 7 : 3(v/v)): 0.79; UV (CHCl<sub>3</sub>)  $\lambda_{\text{max}}$ (nm): 344, IR (KBr)  $\bar{\nu}$  (cm<sup>-1</sup>): 3434 (N–H), 1631 (C=C), 1501 (C=N), <sup>1</sup>H NMR (CDCl<sub>3</sub>, 400 MHz)  $\delta$  (ppm): 9.6 (s, 1H, N–H), 8.37 (s, 1H, Ar–H), 8.1 (d, 1H, <sup>3</sup>*J* = 8 Hz, Ar–H), 7.76–7.95 (m, 3H, Ar–H), 7.61 (m, 3H, Ar–H), 7.52–7.53 (t, 3H, <sup>3</sup>*J* = 7.6 Hz, Ar–H), 7.34–7.38 (m, 6H, Ar–H).

**4.4.7. 2-(3,5-Dimethoxyphenyl)-4,5-diphenyl-1H-imidazole (4g, C<sub>23</sub>H<sub>20</sub>N<sub>2</sub>O<sub>2</sub>).** White powder;  $R_f$  (in petroleum ether : ethylacetate; 7 : 3(v/v)): 0.37; UV (CHCl<sub>3</sub>)  $\lambda_{\text{max}}$ (nm): 344, IR (KBr)  $\bar{\nu}$  (cm<sup>-1</sup>): 3434 (N–H), 1601 (C=C), 1470 (C=N), 1155 (C–O); <sup>1</sup>H NMR (acetone + DMSO-*d*<sub>6</sub>, 400 MHz)  $\delta$  (ppm): 12.9 (s, 1H, N–H), 8.01–8.07 (m, 4H, Ar–H), 7.83–7.88 (m, 5H, Ar–H), 7.78 (d, 2H, <sup>3</sup>*J* = 7.8 Hz, Ar–H), 7.64 (t, 1H, <sup>4</sup>*J* = 2 Hz, Ar–H), 3.31 (s, 6H, OCH<sub>3</sub>).

**4.4.8. 2-(Phenyl)-4,5-bis(4-methoxyphenyl)-1H-imidazole (4h, C<sub>23</sub>H<sub>20</sub>N<sub>2</sub>O<sub>2</sub>).** White powder;  $R_f$  (in petroleum ether : ethylacetate; 7 : 3(v/v)): 0.62; UV (CHCl<sub>3</sub>)  $\lambda_{\text{max}}$ (nm): 344; IR (KBr)  $\bar{\nu}$  (cm<sup>-1</sup>): 3430 (N–H), 1613 (C=C), 1504 (C=N), 1248 (C–O); <sup>1</sup>H NMR (acetone + DMSO-*d*<sub>6</sub>, 400 MHz)  $\delta$  (ppm): 12.7 (s, 1H, N–H), 8.62 (d, 2H, <sup>3</sup>*J* = 7.2 Hz, Ar–H), 7.87–7.97 (m, 7H, Ar–H); 7.80 (d, 1H, <sup>3</sup>*J* = 7.2 Hz, Ar–H), 7.38–7.42 (m, 3H, Ar–H), 4.27 (s, 6H, OCH<sub>3</sub>).

**4.4.9. 2-(4-Methoxyphenyl)-4,5-bis(4-methoxyphenyl)-1H-imidazole (4i, C<sub>24</sub>H<sub>22</sub>N<sub>2</sub>O<sub>3</sub>).** White powder;  $R_f$  (in petroleum ether : ethylacetate; 7 : 3(v/v)): 0.28; UV (CHCl<sub>3</sub>)  $\lambda_{\text{max}}$ (nm): 348, IR (KBr)  $\bar{\nu}$  (cm<sup>-1</sup>): 3426 (N–H), 1612 (C=C), 1507 (C=N), 1261 (C–O); <sup>1</sup>H NMR (acetone + DMSO-*d*<sub>6</sub>, 400 MHz)  $\delta$  (ppm): 12.7 (s, 1H, N–H), 8.53 (d, 2H, <sup>3</sup>*J* = 8.8 Hz, Ar–H), 7.92–7.97 (m, 4H, Ar–H), 7.47 (m, 4H, Ar–H), 7.33 (d, 2H, <sup>3</sup>*J* = 8 Hz, Ar–H), 4.29 (s, 9H, 3OCH<sub>3</sub>).

**4.4.10. 2-(2-Naphthyl)-4,5-bis(4-methoxyphenyl)-1H-imidazole (4j, C<sub>27</sub>H<sub>22</sub>N<sub>2</sub>O<sub>2</sub>).** Cream powder;  $R_f$  (in petroleum

ether : ethylacetate; 7 : 3(v/v): 0.48; UV (CHCl<sub>3</sub>) λ<sub>max</sub>(nm): 360; IR (KBr)  $\bar{\nu}$  (cm<sup>-1</sup>): 3425 (N-H), 1613 (C=C), 1511 (C=N), 1247(C-O); <sup>1</sup>H NMR (DMSO-*d*<sub>6</sub>, 400 MHz) δ (ppm): 12.7 (s, 1H, N-H), 8.56 (s, 1H, Ar-H), 8.22 (d, 1H, <sup>3</sup>J = 8 Hz, Ar-H), 7.96–7.98 (m, 4H, Ar-H), 7.46–7.51 (m, 8H, Ar-H), 6.97 (m, 3H, Ar-H), 3.76 (s, 3H, OCH<sub>3</sub>), 3.69 (s, 3H, OCH<sub>3</sub>).

**4.4.11. 2-(3,4-Dimethoxyphenyl)-4,5-bis(4-fluorophenyl)-1H-imidazole (4k, C<sub>23</sub>H<sub>18</sub>F<sub>2</sub>N<sub>2</sub>O<sub>2</sub>).** Cream powder; R<sub>f</sub> (in petroleum ether : ethylacetate; 7 : 3(v/v)): 0.24; UV (CHCl<sub>3</sub>) λ<sub>max</sub>(nm): 340; IR (KBr)  $\bar{\nu}$  (cm<sup>-1</sup>): 3440 (N-H), 1604(C=C), 1504 (C=N), 1228(C-O); <sup>1</sup>H NMR (DMSO-*d*<sub>6</sub>, 400 MHz) δ (ppm): 12.9 (s, 1H, N-H), 8.19 (d, 2H, <sup>3</sup>J = 8 Hz, Ar-H); 8.05 (m, 4H, Ar-H), 7.78 (t, 2H, <sup>3</sup>J = 8 Hz, Ar-H), 7.58 (m, 3H, Ar-H), 4.34 (s, 3H, OCH<sub>3</sub>), 4.30 (s, 3H, OCH<sub>3</sub>).

**4.4.12. 2-(2-Naphthyl)-4,5-bis(4-fluorophenyl)-1H-imidazole (4l, C<sub>25</sub>H<sub>16</sub>N<sub>2</sub>F<sub>2</sub>).** White powder; R<sub>f</sub> (in petroleum ether : ethylacetate; 7 : 3(v/v)): 0.73; UV (CHCl<sub>3</sub>) λ<sub>max</sub>(nm): 352; IR (KBr)  $\bar{\nu}$  (cm<sup>-1</sup>): 3433 (N-H), 1669 (C=C), 1559 (C=N), 1247(C-O); <sup>1</sup>H NMR (DMSO-*d*<sub>6</sub>, 400 MHz) δ (ppm): 12.9 (s, 1H, N-H), 8.58 (s, 1H, Ar-H), 8.23 (d, 1H, <sup>3</sup>J = 7.2 Hz, Ar-H), 7.94–8.21 (m, 4H, Ar-H), 7.47–7.56 (m, 5H, Ar-H), 7.33 (t, 2H, <sup>3</sup>J = 8.4 Hz, Ar-H), 7.16 (t, 2H, <sup>3</sup>J = 8.4 Hz, Ar-H).

## Acknowledgements

We gratefully acknowledge the financial support from the Research Council of the University of Kashan for supporting this work by Grant (no. 256722/29).

## References

- 1 S. Samai, G. C. Nandi, P. Singh and M. S. Singh, *Tetrahedron*, 2009, **65**, 10155–10161.
- 2 A. Teimouri and A. Najafi Chermahini, *J. Mol. Catal. A: Chem.*, 2011, **34**, 639–645.
- 3 M. Antolini, A. Bozzoli, C. Ghiron, G. Kennedy, T. Rossi and A. Ursini, *Bioorg. Med. Chem. Lett.*, 1999, **9**, 1023–1028.
- 4 K. Sivakumar, A. Kathirvel and A. Lalitha, *Tetrahedron Lett.*, 2010, **51**, 3018–3021.
- 5 J. C. Lee, J. T. Laydon, P. C. McDonnell, T. F. Gallagher, S. Kumar, D. Green, D. McNulty, M. J. Blumenthal, J. R. Keys, S. W. L. Vatter, J. E. Strickler, M. M. McLaughlin, I. R. Siemens, S. M. Fisher, G. P. Livi, J. R. White, J. L. Adams and P. R. Young, *Nature*, 1994, **372**, 739–746.
- 6 A. K. Takle, M. J. B. Brown, S. Davies, D. K. Dean, G. Francis, A. Gaiba, A. W. Hird, F. D. King, P. J. Lovell, A. Naylor, A. D. Reith, J. G. Steadman and D. M. Wilson, *Bioorg. Med. Chem. Lett.*, 2006, **163**, 78–381.
- 7 R. Schmierer, H. Mildenerger and H. Buerstell, German Patent 361464, 1987, Chem. Abstr., 1988, 108, 37838.
- 8 S. E. de Laszlo, C. Hacker, B. Li, D. Kim, M. MacCoss, N. Mantalo, J. V. Pivnichny, L. Colwell, G. E. Koch, M. A. Cascieri and W. K. Hagmann, *Bioorg. Med. Chem. Lett.*, 1999, **96**, 41–646.
- 9 T. Maier, R. Schmierer, K. Bauer, H. Bieringer, H. Buerstell and B. Sachse, U. S. Patent 4820335, 1989, Chem. Abstr., 1989, 111, 19494.
- 10 J. Heeres, L. J. J. Backx, J. H. Mostmans and J. Van Custem, *J. Med. Chem.*, 1979, **22**, 1003–1005.
- 11 A. Shaabani and A. Rahmati, *J. Mol. Catal. A: Chem.*, 2006, **249**, 246–248.
- 12 K. Sivakumar, A. Kathirvel and A. Lalitha, *Tetrahedron Lett.*, 2010, **51**, 3018–3021.
- 13 K. F. Shelke, S. B. Sapkal, S. S. Sonar, B. R. Madje, B. B. Shingate and M. S. Shingare, *Bull. Korean Chem. Soc.*, 2009, **30**, 1057–1060.
- 14 S. D. Jadhve, N. D. Kokare and S. D. Jadhve, *J. Heterocycl. Chem.*, 2009, **45**, 1461–1464.
- 15 H. Weinmann, M. Harre, K. Koeing, E. Merten and U. Tilestam, *Tetrahedron Lett.*, 2002, **43**, 593–595.
- 16 J. Liu, J. Chen, J. Zhao, Y. Zhao, L. Li and H. Zhang, *Synthesis*, 2003, 2661–2666.
- 17 N. D. Kokare, J. N. Sangshetti and D. B. Shinde, *Synthesis*, 2007, 2829–2834.
- 18 M. M. Khodaei, K. Bahrami and I. Kaviani, *J. Chin. Chem. Soc.*, 2007, **54**, 829–833.
- 19 X. Zheng, S. Luo, L. Zhang and J. P. Cheng, *Green Chem.*, 2009, **11**, 455–458.
- 20 (a) A. Maleki, N. Ghamari and M. Kamalzare, *RSC Adv.*, 2014, **49**, 9416–9423; (b) L. Liu, L. Xiao, H. Zhu and X. Shi, *Microchim Acta*, 2012, **178**, 413–419.
- 21 J. Safari, S. H. Banitaba and S. D. Khalili, *J. Mol. Catal. A: Chem.*, 2011, **335**, 46–50.
- 22 G. Chen and B. Fang, *Bioresour. Technol.*, 2011, **102**, 2635–2640.
- 23 (a) M. G. Dekamin, M. Azimoshan and L. Ramezani, *Green Chem.*, 2013, **158**, 811–820; (b) J. Zhu, P. C. Wang and M. Lu, *New J. Chem.*, 2012, **36**, 2587–2592.
- 24 S. Wu, H. Ma, X. Jia, Y. Zhong and Z. Lei, *Tetrahedron*, 2011, **67**, 250–256.
- 25 (a) G. A. Dee, O. Rhode and R. Wachter, *Cosmetics & Toiletries*, 2001, **116**, 39–44; (b) K. R. Reddy, K. Rajgopal, C. U. Maheswari and M. L. Kantam, *New J. Chem.*, 2006, **30**, 1549–1552.
- 26 R. Mohammadi and M. Zaman Kassae, *J. Mol. Catal. A: Chem.*, 2013, **380**, 152–158.
- 27 A. Zhu, L. Yuan and T. Liao, *Int. J. Pharm.*, 2008, **350**, 361–368.
- 28 Z. Liu, H. Bai and D. D. Sun, *New J. Chem.*, 2011, **35**, 137–140.
- 29 J. Safari, S. D. Khalili, S. H. Banitab and H. Dehghani, *Bull. Korean Chem. Soc.*, 2011, **55**, 1–7.
- 30 J. Safari, S. D. Khalili, M. Rezaei, S. H. Banitab and F. Meshkani, *Monatsh. Chem.*, 2010, **141**, 1339–1345.
- 31 S. D. Khalili, and J. Safari, PhD Thesis, Kashan University, Kashan, Iran, 2011.